Specific Triazine Resistance in Bacterial Reaction Centers Induced by a Single Mutation in the Q_A Protein Pocket

Jean-Alexis Spitz, Valérie Derrien, and Pierre Sebban*

Laboratoire de Chimie−Physique, UMR 8000, Bât. 350, Faculté d'Orsay, 91405 Orsay Cedex, France

Received June 23, 2004; Revised Manuscript Received October 4, 2004

ABSTRACT: We report here the first example of a reaction center mutant from *Rhodobacter sphaeroides*, where a single mutation (M266His → Leu) taking place in the primary quinone protein pocket confers selective resistance to triazine-type inhibitors (terbutryn, ametryn, and atrazine), which bind in the secondary quinone protein pocket, at about 13 Å from the mutation site. The M266His → Leu mutation involves one of the iron atom ligands. Interestingly, neither the secondary quinone nor the highly specific inhibitor stigmatellin binding affinities are affected by the mutation. It is noticeable that in the M266His → Ala mutant a nativelike behavior in observed. We suggest that the long side chain of Leu in position M266 may lack space to accommodate in the Q_A pocket therefore transferring its hindrance to the Q_B pocket. This may occur via the structural feature formed by the Q_A−M219His−Fe−L190His−inhibitor (or Q_B) connection, pushing L189Leu and/or L229Ile in closer contact to the triazine molecules, therefore decreasing their bindings. This opens the possibility to finely tune, in reaction center proteins, the affinity for herbicides by designing mutations distant from their binding sites.

Prokaryotic photosynthetic bacteria are the ancestors of the oxygen-evolving organisms, including cyanobacteria. The reaction center (RC)[1] protein from purple photosynthetic bacteria gave rise to photosystem-II-like RC proteins, carrying electron acceptors (such as quinones) of higher midpoint redox potential than the photosystem-I-like RCs. The similarities between bacterial and photosystem II RCs are highlighted by the high sequence homology between their respective core subunits (L and M and D1 and D2, respectively, in bacteria and oxygen-evolving systems) and by the similarities of their three-dimensional protein structures obtained by X-ray crystallography (*1*−*3*).

Absorption of light energy by the antenna surrounding the bacterial RC or directly by RC results in the excitation of the primary electron donor, P (a dimer of bacteriochlorophylls) to its electronic excited state of lowest energy, P*. This very strong electronegative species deactivates by electron donation initiating a transmembrane charge separation between P^+, situated on the periplasmic side of the membrane, and Q_B^-, the secondary quinone acceptor situated on the cytoplasmic side of the membrane. The Q_B-binding protein pocket is provided by the L subunit of the RC. A non-heme iron atom stands close to Q_B (∼10 Å apart) in a position such that the line joining P to the Fe atom is an order of 2 symmetry axis for the protein. The first quinone electron acceptor, Q_A, lies in the M protein in a symmetrical position to Q_B with respect to the iron atom. In *Rhodobacter* (*Rb.*) *sphaeroides*, Q_A and Q_B are both ubiquinone$_{10}$. Interestingly, the three-dimensional structure of the protein shows a symmetrical motif relating Q_A to Q_B through the Fe atom. Indeed, the Fe atom is situated at the interface of the L and M subunits, being coordinated to four His residues, two from the L protein (HisL190 and HisL230) and two from the M protein (HisM219 and HisM266), and to a Glu residue (GluM234). HisL190 and HisM219 develop hydrogen bounds with one carbonyl of Q_A and Q_B, respectively. As presented in Figure 1, this picture can be seen as an extended wire "Q_A−HisM219−Fe−HisL190−Q_B" connecting Q_A to Q_B. This structural feature has previously been proposed to be involved in the functional connection between the two quinone pockets, reported in many experiments (*4*).

Competitive inhibitors for the Q_B site in photosystem II of plants and cyanobacteria are denoted as herbicides because they prevent the Q_A^- to Q_B electron transfer to proceed and therefore are lethal for the photosynthetic growth. Some of these compounds are also active in bacteria. Among those of particular interest are the triazines, because their remanence in the soils and water is harmful for the environment.

Because RCs from purple bacteria are highly homologous to photosystem II RCs of plants (∼40%), they are useful models to investigate the possibility of producing mutants modified in their triazine sensitivity, either designing them by site-directed mutagenesis or by selection on their resistance phenotypes. The three-dimensional structures of RC from *Rhodopseudomonas (Rp.) viridis* containing triazine-type atrazine and terbutryn have been determined (*5*, *6*) (respective PDB entry codes 5PRC and 1DXR). The three-dimensional structures of the RC from the same species have also been obtained with UQ_2 present in the Q_B position or with the very specific inhibitor stigmatellin (*2*) (PDB entry code 4PRC). These data will be used here to interpret our results.

* To whom correspondence should be addressed. E-mail: pierre.sebban@lcp.u-psud.fr. Telephone: 33 (0)6 89 49 23 76. Fax: 33 (0)1 69 15 55 80.

[1] Abbreviations: Q_A, primary quinone; Q_B, secondary quinone; *Rb.*, *Rhodobacter*; RC, reaction center; *Rp.*, *Rhodopseudomonas*; LDAO, lauryldimethylamine *N*-oxide.

10.1021/bi048701m CCC: $30.25
Published on Web 01/04/2005

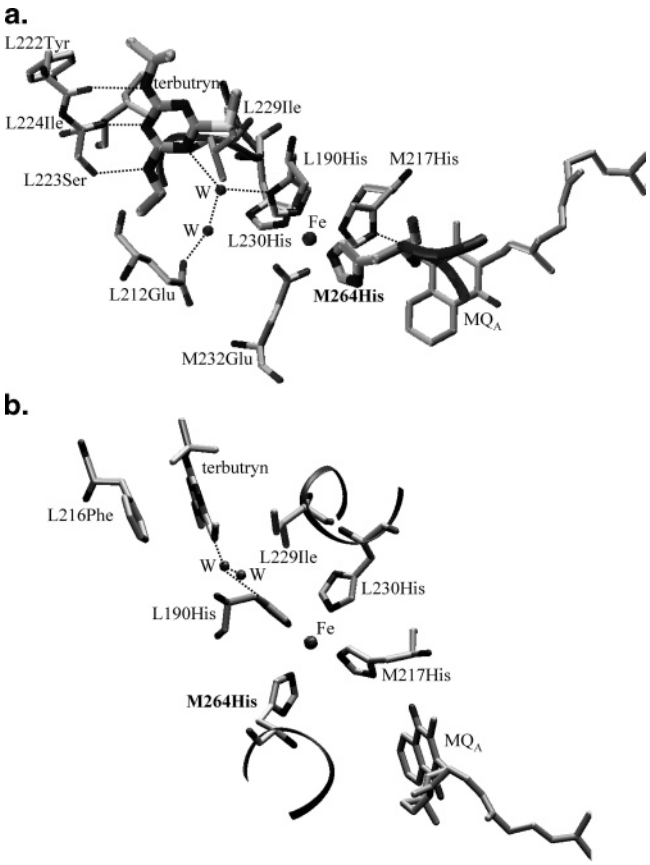

FIGURE 1: Structural scheme of *Rp. viridis* RC (mutant HL168F) containing terbutryn (1DXR) from ref *1*. L168His is situated on the periplasmic side of the complex at about 32 Å from the Fe atom). a and b are rotated by 90°. The dotted lines represent the hydrogen bonds as described in ref *5*. M264His and M217His in *Rp. viridis* are respectively numbered M266His and M219His in *Rb. sphaeroides*.

The majority of RC mutants reported so far as herbicide/inhibitor-resistant variants contain amino acid modifications in the Q_B-binding pocket. This has previously been reported for *Rb. sphaeroides* (*7*), *Rb. capsulatus* (*8*), and *Rp. viridis* (*9*−*11*). However, reports have shown that in *Rhodospirillum rubrum* RC, mutation M234Glu → Lys confers resistance to different types of inhibitors including NH-thiazoles and terbutryn (*12*). In *Rb. sphaeroides* RCs, the M234Glu → Arg and M234Glu → Lys mutations also confer notable resistance to terbutryn (Vaillet, V., Master's diploma and Hanson, D. K., Schiffer, M., Vaillet, V., and Sebban, P., unpublished data). As shown in Figure 1, M234Glu is situated halfway from Q_A and Q_B.

We report here a further more remarkable effect. Upon mutation of M266His → Leu (situated on the other side of the iron atom in regard to Q_B at a distance of about 15 Å), a specific resistance to triazines is induced. Thanks to the investigation of these effects on isolated RC proteins at room temperature, we have determined the K_i values for three types of triazine molecules and compared them to the wild-type (WT) values. Interestingly, neither the K_i value for the highly specific inhibitor stigmatellin nor the K_M value for the quinone itself in the Q_B site is affected by the mutation.

MATERIAL AND METHODS

Mutant Construction and Growth Conditions. A *Sma*I 1.3-kb DNA fragment containing the M266H (histidine) codon of the *Rb. sphaeroides puf M* gene has been isolated from the pRK 5.3 plasmid (*13*) containing the entire *puf* operon from *Rb. sphaeroides* (*14*). The 1.3-kb fragment is ligated into the *Sma*I restriction site of pBluescript SK (Stratagene). This plasmid called pBS1.3 is used to perform mutagenesis of the M266H residue. To direct the mutagenesis, the oligonucleotides 5′-TCAACGCCACGATGGAAGGCATCGCG-CGCTGGGCCATCTGG-3′ and 5′-TCAACGCCACGATG-GAAGGCATCCTGCGCTGGGCCATCTGG-3′ for the M266HA and M266HL mutants, respectively, were synthesized (Genosys−Sigma). The mutated codons are underlined. The mutations were incorporated into the *puf M* gene of pBS1.3 using the Quick-Change mutagenesis kit (Stratagene). Sequence analysis confirmed that the desired mutations and no others were within the 742-base-pair (bp) region around the mutation site. The sequenced 742-bp fragment comprising the M266 mutation was then isolated by double digestion with *Aat*II and *Bst*XI and cloned into the pBS5.3Δ*Bst*XI plasmid (*Bst*XI restriction site deleted from the polylinker region) containing the entire WT *puf* operon from *Rb. sphaeroides* (a 5.3-kb *Hin*dIII−*Bam*HI fragment). The 5.3-kb *Hin*dIII−*Bam*HI fragment carrying the M266HA or M266HL mutation was recloned into pRK404, transformed into *Escherichia coli* S17-1 (*15*) and used to complement the *Rb. sphaeroides puf* ΔLMX21 (*16*).

Rb. sphaeroides WT and mutant strains harboring *puf M* mutation on PRK404 were grown in Erlenmeyer flasks filled to 50% of the total volume with malate yeast medium supplemented with kanamycin (20 μg/mL) and tetracycline (4 μg/mL). The cultures were grown in darkness at 30 °C on a gyratory shaker (140 rpm).

The RC purification was achieved as previously described (*17*).

RESULTS

Q_B-Binding Affinity. The binding of Q_B in RCs is described by the equilibrium

$$[RC] + [Q] \underset{k_{off}}{\overset{k_{on}}{\rightleftharpoons}} [RC]_{Q_B} \qquad (1)$$

where $K_M = k_{off}/k_{on}$, represents the dissociation constant for Q_B. [RC], [Q], and $[RC]_{Q_B}$ are the concentrations of RCs with an empty Q_B pocket, of free quinone, and of RCs with bound Q_B, respectively

The activity of the enzyme (RC) in regard to quinone (substrate) binding can be defined as

$$\text{activity} = \%Q_B = \frac{[RC]_{Q_B}}{[RC]_{total}} = \frac{[Q]}{[Q] + K_M} \qquad (2)$$

where $[RC]_{total} = [RC] + [RC]_{Q_B}$.

In our measurements, where the added quinone concentration is much higher than the total RC concentration ($[RC]_{total}$), the total (added) quinone concentration is nearly the same as the free quinone concentration, i.e., $[Q]_{total} \sim [Q]$. Therefore, the Q_B site activity is described by

$$\text{activity} = \%Q_B = \frac{[RC]_{Q_B}}{[RC]_{total}} = \frac{[Q]_{total}}{[Q]_{total} + K_M} \qquad (3)$$

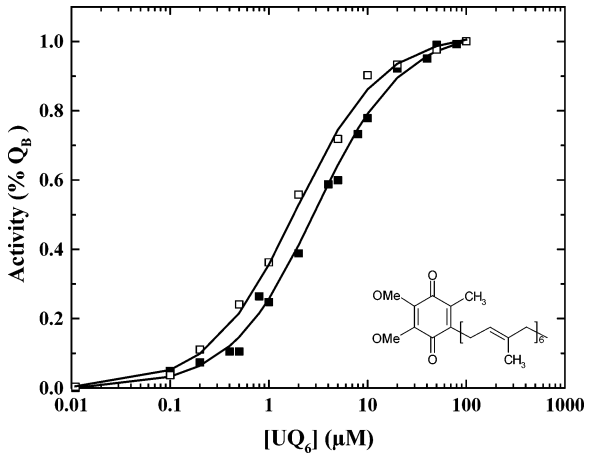

FIGURE 2: Quinone (UQ_6) titration of the secondary quinone activity in the RCs (0.5 μM) from the WT (■) *Rb. sphaeroides* and the M266HL mutant (□). The lines are drawn according to eq 3. The K_M values obtained are respectively 3.0 ± 0.3 and 1.9 ± 0.3 μM. The RCs (0.5 μM) were suspended in 10 mM Tris-HCl buffer at pH 7.8 and 0.05% LDAO. T = 21 °C.

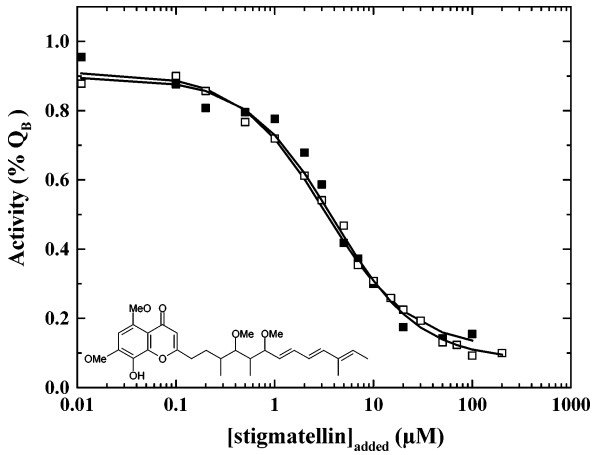

FIGURE 3: Secondary quinone (UQ_6) activity inhibition curves for stigmatellin in the RCs from the WT (■) *Rb. sphaeroides* and the M266HL RC mutant (□). The lines are drawn by fitting the data with eq 4. The derived dissociation constants for stigmatellin are 0.18 ± 0.05 μM for the WT and 0.18 ± 0.05 μM for the mutant. The RCs (0.5 μM) were suspended in 10 mM Tris-HCl buffer at pH 7.8 and 0.05% LDAO. T = 21 °C. The UQ6 concentration was 30 μM.

$[RC]_{Q_B}$ has been determined by the relative amplitude of the $P^+Q_B^-$ charge recombination, which reflects the population of RCs that are Q_B-bound.

For the WT and mutant RCs, this amplitude is easily distinguishable from that characteristic of the $P^+Q_A^-$ recombination. Indeed, at pH 7.8, where all experiments were achieved, in the WT, these two rates are 9.4 and 0.95 s^{-1} for the $P^+Q_A^-$ and $P^+Q_B^-$ recombination processes, respectively. In the mutant, these rates are 8.1 and 0.3 s^{-1}, respectively.

Figure 2 shows the Q_B-binding titration curves in the RCs from the WT and M266HL mutant. The K_M values derived by fitting these curves with eq 3 are 3 ± 0.2 and 1.9 ± 0.2 μM for the WT and M266HL mutant RCs, respectively. The WT value is close to that previously determined (*7*). The M266His → Leu mutation has not notably modified this value.

Inhibitor-Binding Affinities. In the presence of competitive inhibitors (I) of the Q_A^- to Q_B electron transfer, which displace the binding of Q_B in its site, eq 1 becomes (*7*, *8*)

$$[RC]_i \underset{k_{-i}}{\overset{k_i}{\rightleftharpoons}} [I] + [RC] + [Q] \underset{k_{off}}{\overset{k_{on}}{\rightleftharpoons}} [RC]_{QB} \qquad (3)$$

where $K_i = k_i/k_{-i}$ represents the dissociation constant for I and [I] represents the concentration of the free inhibitor. Because $[RC]_{total}$ is small compared to [I] in the titrations, we shall assume that $[I] \sim [I]_{total}$, the total or added inhibitor concentration. Therefore, eq 4 accounts for the $\%Q_B$ in the presence of the competitive inhibitor

$$\text{activity} = \%Q_B = \frac{[RC]_{QB}}{[RC]_{total}} = \frac{[Q]_{total}}{[Q]_{total} + K_M + \frac{K_M}{K_i} \times [I]_{total}} \qquad (4)$$

The inhibition titration curve for stigmatellin is presented in Figure 3. The WT and mutant titrations are nearly superimposable within the experimental error. The K_i values for the WT and M266HL RC mutant derived by fitting these curves with eq 4 lead to respective values of 0.18 ± 0.05 and 0.14 ± 0.05 μM. Therefore, the mutation does not change the affinity of the RC protein for stigmatellin.

Figure 4 presents the inhibition curves for the three triazine inhibitors, terbutryn, ametryn, and atrazine. Their respective chemical structures are presented in the inset.

The K_i values evaluated from the fits of the curves of Figure 4 are presented in Table 1.

The K_i value for terbutryn (~27 μM) is substantially increased compared to that of the WT (~1.6 μM). The ametryn resistance induced by the M266HL mutation is about 9 times ($K_i \sim 27$ μM versus 3 μM for the WT). In the case of atrazine, the effect is less pronounced (about a 2 times increase of K_i in the mutant). However, the WT RCs from *Rb. sphaeroides* have previously been shown as only weakly sensitive to atrazine, at variance to *Rb. capsulatus* (*18*). The weaker increase effect of atrazine resistance in the M266HL mutant as compared to the WT is therefore still noticeable.

DISCUSSION

We show here the first example of a single mutation (M266His → Leu) pointing toward the Q_A protein pocket of the RCs, which notably reduces the binding of triazines in the Q_B pocket. This effect is further remarkable in the way that the binding affinities for the Q_B and stigmatellin molecules are essentially not changed. The mutation site per se is probably less of an important factor than the point mutation itself because, in the M266HA mutant, the binding affinities for Q_B, stigmatellin, and triazines are essentially not changed compared to those of the WT (Table 1).

Three crystallographic studies achieved in *Rp. viridis* RCs, one on the binding of Q_B and stigmatellin (*2*) and two on the respective bindings of atrazine and terbutryn (*5*, *6*), are relevant to our results. Even achieved on a different protein, the high protein sequence homology that exists between *Rb. sphaeroides* and *Rp. viridis* in the binding region of the quinones allows us to use these structures to help us understand our data. Furthermore, the similar relative binding

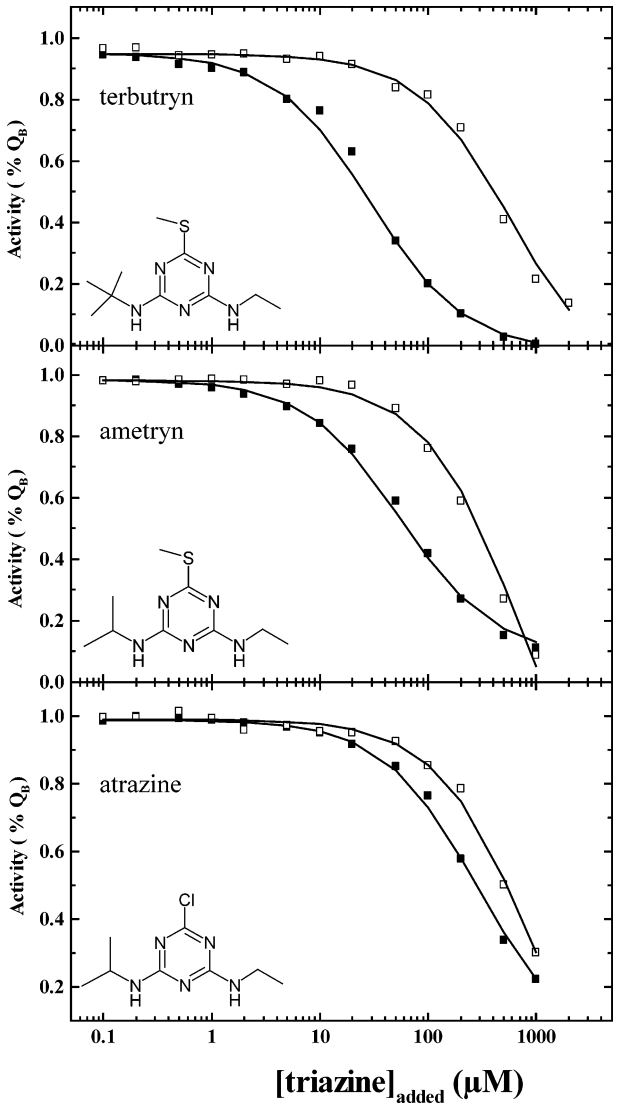

FIGURE 4: Secondary quinone (UQ_6) activity inhibition curves for terbutryn, ametryn, and atrazine in the RCs from the WT (■) *Rb. sphaeroides* and the M266HL RC mutant (□). The lines are drawn by fitting the data with eq 4. The derived dissociation constants for terbutryn are 1.6 ± 0.3 μM for the WT and 27 ± 2 μM for the M266HL mutant. For ametryn, K_i = 3 ± 0.3 and 27 ± 3 μM for the WT and mutant, respectively. For atrazine, K_i = 15.5 ± 1 and 30 ± 2 μM for the WT and mutant, respectively. The RCs (0.5 μM) were suspended in 10 mM Tris-HCl buffer at pH 7.8 and 0.05% LDAO. T = 21 °C. The UQ6 concentration was 30 μM.

affinities for the three kinds of molecules (ubiquinone, stigmatellin, and triazines) measured in both strains supports the reliability of the comparison between the Q_B-binding pocket in *Rp. viridis* and *Rb. sphaeroides* RCs.

Structural (*1*, *19*, *20*) and theoretical studies (*2*, *21*) have previously suggested that two binding sites can be occupied by Q_B in the RCs. The distal (from the Fe atom) and proximal sites are distant from about 5 Å and involve a 180° rotation of the quinone ring. According to recent FTIR measurements (*22*, *23*), it appears that the functional site, which is occupied by Q_B most of the time, is the proximal position either in the dark or under illumination of the RCs. In addition, it has also been suggested by numerical calculations that, even if Q_B has some probability to be in the distal site in the dark, the formation of Q_A^- pushs it toward the proximal site (*24*). For these reasons and because the quinone-binding affinities determined here are achieved by titrating the relative amplitudes of the $P^+Q_A^-$ and $P^+Q_B^-$ charge recombinations (Q_A^- present), i.e., in the presence of Q_A^-, the structural interpretations of our data are based on a proximal binding site occupation of Q_B.

Structural Data. In the structural works of Lancaster and Michel (*2*, *6*) and Lancaster et al. (*5*), different types of interactions are pointed out to be of importance for the binding energy of Q_B and inhibitors in the Q_B protein pocket. We describe them shortly below.

The respective three-dimensional structures of the RCs with UQ_2 acting as Q_B (proximal site) and with stigmatellin in the Q_B site show similar binding interactions (*2*).

The hydrogen-binding patterns constitute the first set of important interactions contracted by these molecules with the protein.

In the proximal site, Q_B develops three main hydrogen bonds. One is provided by the Nδ of L190His to the O4 carbonyl oxygen of Q_B. The two others are developed between the O1 carbonyl oxygen of Q_B and the backbone peptide nitrogens of L224Ile and L225Gly.

Stigmatellin is suggested to bind in the same proximal domain of the pocket with a similar hydrogen-binding pattern. However, the stronger binding for this inhibitor probably arises from the presence of two additional hydrogen bonds. The first one is developed between the Oγ atom of L223Ser and the hydroxyl group of stigmatellin (*2*). The importance of this interaction is highlighted by the fact that, in *Rb. sphaeroides*, the L223SA single mutant is resistant to stigmatellin (*25*). The other additional bond developed by stigmatellin arises from the doubling of the hydrogen bond from the Nδ of L190His to the proximal methoxy oxygen of stigmatellin.

Atrazine and terbutryn bind in a more distal position (*5*, *6*) of the Q_B pocket. This allows the presence of two firmly bound water molecules (absent in the presence of Q_B or stigmatellin), one of which develops a hydrogen bond (donor) with the N1 of the triazine ring on one side and an hydrogen bond (acceptor) with the Nδ of L190His on the other side. The N5 of the triazine ring and the N11 and N7 of triazines respectively develop hydrogen bounds with the N peptide of L224Ile, the carbonyl O of L222Tyr, and the Oγ atom of L223Ser. Thus, four hydrogen bonds are developed by the triazine molecules under their bindings.

Another factor of importance for the binding of Q_B and inhibitors is the presence of L216Phe and especially the orientation of its ring compared to that of Q_B or the inhibitors (*6*, *10*, *11*). Indeed, it has been suggested that the interactions between the π electronic orbitals of both rings (L216Phe and Q_B/inhibitors) notably contribute to the stability of the Q_B/inhibitors in the protein pocket. The quinone and the chromone rings of stigmatellin have similar orientations differening by ~9° in regard to the phenyl ring of L216Phe (*2*). At variance, the ring of atrazine is tilted and makes an angle of 24° with the phenyl ring of L216Phe (*6*), whereas this angle is 17° in the case of terbutryn (*5*). The difference between the two triazines orientations may only partly account (5) for the higher dissociation constant of atrazine as compared to terbutryn in RCs of *Rb. capsulatus* (*18*) and measured here in the WT *Rb. sphaeroides*. Indeed, as suggested in ref *6*, the slightly different contacts of terbutryn and atrazine with the protein, because of their different

Table 1: Dissociation Constant Values for Ubiquinone 6, Stigmatellin, and Triazines Measured at pH 7.8 in the RCs from WT *Rb. sphaeroides* and the M266HL Mutant

	UQ_6 K_M (μM)	stigmatellin K_i (μM)	terbutryn K_i (μM)	ametryn K_i (μM)	atrazine K_i (μM)
WT	3.0 (±0.3)	0.18 (±0.05)	1.6 (±0.3)	3 (±0.3)	15.5 (±1.0)
M266HL	1.9 (±0.3)	0.14 (±0.05)	27 (±2)	27 (±2)	30 (±2)
M266HA	2.8 (±0.3)	0.15 (±0.05)	1.8 (±0.3)	2.7 (±0.3)	16 (±1.0)
$K_{iM266HL}/K_{iWT}$		~0.8	~16	~9	~2

specific lateral groups (methylthio versus chloro), develop different van der Waals contacts with L189Leu and L229Ile. This may also account for the different atrazine-binding affinities.

Understanding of the Induced Triazine Resistance in the M266HL Mutant. The nearly unchanged binding affinities for Q_B and stigmatellin in the RC from the M266HL mutant are consistent with their similar binding properties in the WT. Indeed, it seems unlikely that the binding of only one of the two compounds (Q_B or stigmatellin) could be specifically modified. Our data suggest that none of the important interactions for their respective bindings, i.e., the orientation of their rings (in regard to L216Phe) and the strength of the hydrogen bonds that they develop with the protein has been modified by the mutation. The specific resistance to stigmatellin in the L223SA mutant (*25*) is a good example of the strong effect of the loss of only one hydrogen bond.

Therefore, the functional data presented here suggest that neither of the hydrogen bonds developed by Q_B nor by stigmatellin (or both) with L190His, L224Ile, L225Gly, and L223Ser have been modified by the M266HL mutation. That is not the case for the triazines.

As mentioned above, in the WT, triazines do not bind with the same affinities. Indeed, for terbutryn, ametryn, and atrazine, the evaluated K_i values are respectively, 1.6, 3, and 15.5 μM (Table 1). As suggested by Lancaster et al. (*5*), the looser binding of atrazine may arise from the hindrance of the van der Waals contacts (chloro versus methylthio/thio groups for terbutryn and ametryn) with the side chain of L189Leu and L229Ile. To check this hypothesis, we have measured the dissociation constant for terbutryn in RC single mutants from *Rb. capsulatus* (a kind gift from E. Bylina) modified at position L229Ile (*26*). In the case of the longer side chain as Met, the dissociation constant for terbutryn in the L229IM mutant is 10-fold increased compared to that of the WT. Conversely, when short side chains are present in position L229, the K_i value for terbutryn is decreased by a factor of 3 in the case of Val (L229IV mutant) and as much as 30 times in the case of Ala (L229IA mutant). These strong variations, which seem to be related to the length of the side chain, demonstrate the very high sensitivity of the K_i values for triazines upon their van der Waals contacts with L229Ile.

In the M266HL mutant, the notable reduction of the binding of the triazines may be understood under the light of their different binding patterns in a distal position of the Q_B site.

As observed in the WT, the angle between the L216Phe side chain and the ring of either terbutryn (~17°), atrazine (24°), quinone (9°), or stigmatellin (9°) does not seem to be strongly related to the dissociation constant of these molecules. We therefore do not favor that a notable change in the mutant of these $\pi-\pi$ interactions between triazines and the phenyl group may explain the triazine decreased binding in the mutant.

The unmodified dissociation constant for Q_B and stigmatellin in the M266HL mutant also eliminates the hypothesis of any notable modification of the side chain orientation or movement of the backbone carbons of L223Ser or L224Ile. Consequently, it seems unlikely that changes in the hydrogen-bond strength between the triazines and these two residues may have been affected by the M266HL mutation. Because L222Tyr is further away in the pocket, it seems also unlikely that the hydrogen bond between its O carbonyl and the N11 of terbutryn may have been modified in the mutant.

Thus, the most likely structural modification in the mutant to account for the specific binding decrease for triazines is more a change in the presence or position of the water molecule, which hydrogen binds the N1 of the triazine ring and the Nδ of L190His, or alternatively a slight movement of L229Ile and/or L189Leu toward the triazine molecules.

We are currently trying to determine the structures of the RCs from the M266HL and M266HA mutants (Koepke, J., Linhard, V., Derrien, V., Sebban P., and Fritzsch, G., unpublished data). The preliminary data indicate that the replacement of M266H does not affect the Fe content in the protein (Koepke, J., Linhard, V., Derrien, V., Sebban P., and Fritzsch, G., unpublished data). However, the current low resolution of the structure of the M266HL RC mutant (~3.3 Å) cannot tell us yet if any change occurs in the Q_B pocket. The better resolution (~2.6 Å) in the M266HA RC mutant suggests a small displacement of the Fe toward the Q_B pocket.

Thus, we do not consider as likely a change in the hydrogen-bond pattern involving the above-considered water molecules. When the very high influence of the van der Waals contacts between the side chain in position L229Ile and the triazines on the K_i value is taken into account, we favor the hypothesis that L229Ile and/or L189Leu have been pushed toward the lateral groups of triazines in the M266HL mutant.

It is of interest to note that the K_i values measured in the mutant are the same for the three triazine inhibitors, suggesting that the structural feature, which reduces their binding, dominates all other interactions as a "binding limiting factor".

The absence of the resistance effect in the M266HA RC mutant suggests that the long side chain of Leu in position M266 may lack space to accommodate in the Q_A pocket, therefore passing on this hindrance to the Q_B pocket.

Our study opens the possibility to predict (with the help of numerical calculations) and design new types of RC mutant proteins in which the affinities of inhibitors or drugs are more finely tuned by mutations distant from their binding site.

ACKNOWLEDGMENT

We thank Dr. Laura Baciou for careful reading of the manuscript.

REFERENCES

1. Stowell, M. H., McPhillips, T. M., Rees, D. C., Soltis, S. M., Abresch, E., and Feher, G. (1997) Light-induced structural changes in photosynthetic reaction center: Implications for mechanism of electron−proton transfer, *Science 276*, 812−816.
2. Lancaster, C. R., and Michel, H. (1997) The coupling of light-induced electron transfer and proton uptake as derived from crystal structures of reaction centres from *Rhodopseudomonas viridis* modified at the binding site of the secondary quinone, Q_B, *Structure 5*, 1339−1359.
3. Kamiya, N., and Shen, J. R. (2003) Crystal structure of oxygen-evolving photosystem II from *Thermosynechococcus vulcanus* at 3.7 Å resolution, *Proc. Natl. Acad. Sci. U.S.A. 100*, 98−103.
4. Baciou, L., and Sebban, P. (1995) Heterogeneity of the quinone electron acceptor system in bacterial reaction centers, *Photochem. Photobiol. 62*, 271−278.
5. Lancaster, C. R., Bibikova, M. V., Sabatino, P., Oesterhelt, D., and Michel, H. (2000) Structural basis of the drastically increased initial electron transfer rate in the reaction center from a *Rhodopseudomonas viridis* mutant described at 2.00 Å resolution, *J. Biol. Chem. 275*, 39364−39368.
6. Lancaster, C. R., and Michel, H. (1999) Refined crystal structures of reaction centres from *Rhodopseudomonas viridis* in complexes with the herbicide atrazine and two chiral atrazine derivatives also lead to a new model of the bound carotenoid, *J. Mol. Biol. 286*, 883−898.
7. Paddock, M. L., Rongey, S. H., Abresch, E. C., Feher, G., and Okamura, M. Y. (1988) Reaction centers from three herbicide-resistant mutants of *Rhodobacter sphaeroides* 2.4.1: Sequence analysis and preliminary characterization, *Photosynt. Res. 17*, 75−96.
8. Baciou, L., Bylina, E. J., and Sebban, P. (1993) Study of wild type and genetically modified reaction centers from *Rhodobacter capsulatus*: Structural comparison with *Rhodopseudomonas viridis* and *Rhodobacter sphaeroides*, *Biophys. J. 65*, 652−660.
9. Sinning, I. (1992) Herbicide binding in the bacterial photosynthetic reaction center, *Trends Biochem. Sci. 17*, 150−154.
10. Sinning, I., Michel, H., Mathis, P., and Rutherford, A. W. (1989) Characterization of four herbicide-resistant mutants of *Rhodopseudomonas viridis* by genetic analysis, electron paramagnetic resonance, and optical spectroscopy, *Biochemistry 28*, 5544−5553.
11. Baciou, L., Sinning, I., and Sebban, P. (1991) Study of Q_B^- stabilization in herbicide-resistant mutants from the purple bacterium *Rhodopseudomonas viridis*, *Biochemistry 30*, 9110−9116.
12. Sopp, G., Rutherford, W. A., and Oettmeier, W. (1997) A single mutation in the M-subunit of *Rhodospirillum rubrum* confers herbicide resistance, *FEBS Lett. 409*, 343−346.
13. Farchaus, J. W., and Oesterhelt, D. (1989) A *Rhodobacter sphaeroides* puf L, M, and X deletion mutant and its complementation in trans with a 5.3 kp puf operon shuttle fragment, *EMBO J. 8*, 47−54.
14. Zhu, Y. S., Kiley, P. J., Donohue, T. J., and Kaplan, S. (1986) Origin of the mRNA stoichiometry of the puf operon in *Rhodobacter sphaeroides*, *J. Biol. Chem. 261*, 10366−10374.
15. Simon, R., Priefer, U., and Pfihler, A. (1983) A broad host range mobilization system for *in vivo* genetic engineering: Transposon mutagenesis in Gram-negative bacteria, *BioTechnology 1*, 784−791.
16. Davis, J., Donohue, T. J., and Kaplan, S. (1988) Construction, characterization, and complementation of a puf-mutant of *Rhodobacter sphaeroides*, *J. Bacteriol. 170*, 320−329.
17. Gerencser, L., Taly, A., Baciou, L., Maroti, P., and Sebban, P. (2002) Effect of binding of Cd^{2+} on bacterial reaction center mutants: Proton transfer uses interdependent pathways, *Biochemistry 41*, 9132−9138.
18. Ginet, N., and Lavergne, J. (2001) Equilibrium and kinetic parameters for the binding of inhibitors to the Q_B pocket in bacterial chromatophores: Dependence on the state of Q_A, *Biochemistry 40*, 1812−1823.
19. McAuley, K. E., Fyfe, P. K., Cogdell, R. J., Isaacs, N. W., and Jones, M. R. (2000) X-ray crystal structure of the YM210W mutant reaction centre from *Rhodobacter sphaeroides*, *FEBS Lett. 467*, 285−290.
20. Kuglstatter, A., Ermler, U., Michel, H., Baciou, L., and Fritzsch, G. (2001) X-ray structure analyses of photosynthetic reaction center variants from *Rhodobacter sphaeroides*: Structural changes induced by point mutations at position L209 modulate electron and proton transfer, *Biochemistry 40*, 4253−4260.
21. Taly, A., Sebban, P., Smith, J. C., and Ullmann, G. M. (2003) The position of Q_B in the photosynthetic reaction center depends on pH: A theoretical analysis of the proton uptake upon Q_B reduction, *Biophys. J. 84*, 2090−2098.
22. Breton, J., Boullais, C., Mioskowski, C., Sebban, P., Baciou, L., and Nabedryk, E. (2002) Vibrational spectroscopy favors a unique Q_B binding site at the proximal position in wild-type reaction centers and in the Pro-L209 → Tyr mutant from *Rhodobacter sphaeroides*, *Biochemistry 41*, 12921−12927.
23. Nabedryk, E., Breton, J., Sebban, P., and Baciou, L. (2003) Quinone (Q(B)) binding site and protein stuctural changes in photosynthetic reaction center mutants at Pro-L209 revealed by vibrational spectroscopy, *Biochemistry 42*, 5819−5827.
24. Zachariae, U., and Lancaster, C. R. (2001) Proton uptake associated with the reduction of the primary quinone Q(A) influences the binding site of the secondary quinone Q(B) in *Rhodopseudomonas viridis* photosynthetic reaction centers, *Biochim. Biophys. Acta 1505*, 280−290.
25. Paddock, M. L., Feher, G., and Okamura, M. Y. (1995) Pathway of proton transfer in bacterial reaction centers: Further investigations on the role of Ser-L223 studied by site-directed mutagenesis, *Biochemistry 34*, 15742−15750.
26. Bocek, J. (1999) Study of reaction center mutants from the photosynthetic purple bacterium *Rhodobacter capsulatus* modified in their herbicide binding affinities, university thesis, University of Paris XI, Orsay, France/University Charles, Prague, Czech Republic.

BI048701M